AUTOMATIC DETERMINATION OF PHOTOELASTIC PARAMETERS OF PILLAR SCREW

Cleudmar Amaral de Araújo – cleudmar@mecanica.ufu.br
Gualter Aurélio Alves de Souza - gualtersouza@gmail.com
Denize Vilela Novais – denizemecanica@yahoo.com.br
Federal University of Uberlândia, School of Mechanical Engineering. Av. João Naves de Ávila, 2121 – Bl. 1M, Uberlândia, Minas Gerais, CEP: 38400-089, Brazil

Flávio Domingues Neves – neves@triang.com.br
Federal University of Uberlândia, School of Odontology, Av. Rondon Pacheco, 1415, Uberlândia, Minas Gerais, CEP: 38400-089, Brazil

Abstract. *Photoelasticity is an experimental technique used for getting solution for complex engineering problems, especially when analytical and numeric solution is difficult to apply. Photoelasticity is also used for study the stress distribution when the geometry or load distribution is complex. One difficult to application of this technique is that the photoelastic parameters are obtained by direct reading. The direct reading depends on large experience and demands an expensive time for analysis and solution. The main objective of this work is to develop software that gets the photoelastic parameter by an automatizated process. This method uses elliptical polarized light and a calibration model for fringe order analysis and another calibration model for main stress direction. The photoelastic model images are digitalized and treated by the software. The model images are got by use of the elliptical polarized light, and the principal stress are obtained. To validate this technique, is used a disc under load compression. The fringe order analysis is possible by using a calibration model made of the same material of the disc. This calibration model is a bar, loaded by pure bending, and was used for RGB values of different fringe orders. The principal stress directions analysis is possible by using a calibration disc model made of the same photoelastic material.*

Keywords*: Photoelasticity, Stress, Experimental analysis, Photoelastic images, Photoelastic parameters.*

1. Introduction

The mechanical systems design involves two basic steps of development: theoretical and experimental analysis. With the improvement in computational techniques, the theoretical analysis gained special value to the design and development engineering, as well because it is very common that experimental analysis involves high costs. The experimental analysis is justified for the components of complex systems, and it is possible that it be applied under orientation of computational modeling techniques. This approach is common when the solutions for specific and complex problems results in low reliability because the high number of simplifications adopted.

Photoelasticity is an experimental technique for stress/strain analysis of engineering structures, especially of complex models. The technique is an efficient method of whole field analysis for plane or three-dimensional state. In the transmission photoelasticity, it is necessary to made transparent models with birefringent characteristics when loaded mechanically. It is necessary to use an optical equipment called polariscope for use of this technique, which main feature is to work with polarized light. It give us the visualization of photoelastics parameters, in colored fringes, when it is used white light, or black and white fringes, when monochromatic light is used. This order fringe is associated with the stress state of model.

Several authors have developed methods for treat the optical phenomenon of polarized light, like Theocaris P. S., Gdoutos E. E., 1979. The several forms of polarized light are defined by curves that the final point of the light vector passes in the propagation wave. Menges (1940) and Stokes (1852) proved that a defined kind of polarized light can be described by four parameters. These parameters are 4-elements of a vector, called Stokes vector. The Stokes parameters have intensity dimension that can be operationally defined by intensity of emerging light, obtained by use of proper polarizer filters.

In this work, a software in Matlab® environment was developed and it was applied to the acquisition and treatment photoelastics models images aiming at to get the fringes orders and principal stress directions of models submitted to a stress field. The images of the photoelastic models had been obtained by a connected digital camera directly to the polariscope. The technique that uses white light with elliptical polarization is presented, like developed by Yoneyama and Takashi (1998). In the determination of the fringes orders, it was used a four points bending device to obtain a calibration table of a beam photoelastic model under bending conditions. With this, the main objective of the work was to automatize the reading process, acquisition and treatment of the photoelastics parameters aiming at to improve the precision of the results and to facilitate the application of the transmission photoelasticity.

2. Plane transmission photoelasticity

The photoelasticity technique is based in the optical property of some transparent plastic materials that presents different refraction indexes when submitted to a stress/strain condition (Dally and Rilley, 1978).

The use of filters positioned between the observer, the light source and the model, give us the visualization of this phenomenon. These filters are parts of the polariscope, equipment that polarizes the light that passes through it. The polarized light turns possible the observation of the stress by images interpretation which compose the optical parameters (Araújo et. al., 2004).

2.1. The optical relations in the photoelasticity

The Maxwell electromagnetic theory shows that the light is an electromagnetic upset and it can be expressed like a normal vector to the propagation direction. The principal optical effects in photoelasticity can be described like a simple sine wave, in the positive direction of the z axes, like showed in the figure 1. Then, the light propagation in the z direction, represented by,

$$E = f(z - ct) = A\cos\frac{2\pi}{\lambda}(z - ct) \tag{1}$$

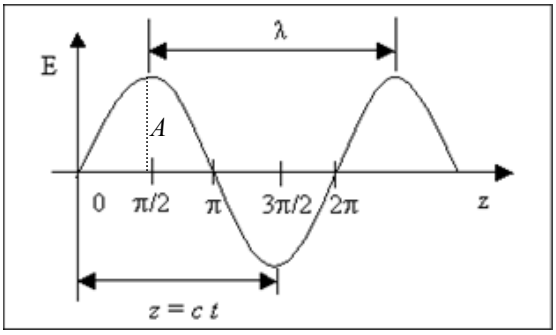

Figure 1. Vector light amplitude depending of axis position.

2.2. Polarized Light

The vibration associated with the light is perpendicular to the propagation direction. A light source emits waves contends transversal vibrations to the propagation direction. With the introduction of a polarizing filter (P) in the light waves way, only one of these vibrations components will be transmitted (that parallel to the polarization axis of the filter). This guided beam is called polarized light. If another polarizing filter (Q) is placed in its trajectory, a complete extinguishing of the beam can be obtained if the polarization axis of the two polariscopes is perpendicular between themselves. The white light, whose waves vibrate in all directions, when passing through the polarizers, is polarized on different lengths, i.e., in different colors. For example, the wavelength (λ) of 400 to the 450 nm corresponds to the violet light and the wavelength (λ) of 630 to the 700 nm corresponds to the red light.

The Brewster law determines that the change of the refractive index is proportional to the difference between principal deformations (Dally and Rilley, 1978). By using this formularization the basic relation for the measure of deformation can be obtained, in terms of the principal stresses, called of stress-optic law, being given by:

$$\sigma_1 - \sigma_2 = \frac{NK\sigma}{b} \tag{2}$$

In The Equation (2) (K_σ) is the constant optic of the material, (N) is the fringe order and (b) the model thickness. When the two waves emerge from the model they are not simultaneous, due to the relative delay (δ), and if this model is between two polarization lenses, the analyzer will only transmit a waves component, which will intervene themselves, and the intensity of resultant light, will be a function of the relative delay (δ) and the polarization axis angle of the analyzer and the principal stresses direction.

2.3. Photoelastic parameters

The interference caused by the phase among light beams that propagating in the two main directions and the angle between the main directions and the polariscope polarization axis give origin the two photoelastic parameters that can be measured.

The angle between the polarization direction and main directions is called isoclinic parameter, that is the geometric places of model points that possess the same direction of the principal stresses, and these coincide with the polariscope polarization directions. They are black curves (where the complete extinguishing of the light occurs) that appear in the analyzer of a plan polariscope and its value can be determined by turning the polarizer/analyzer set in relation to the model. They are necessary to localize the principal stresses direction.

The phase angle between the vectors light and the principal stresses directions is called isocromatics parameters, and they are the geometric places of the model points, which have the same direction of the main stresses, and these coincide with the polariscope polarization directions. This parameter is easily identified in the circular polariscope, which has the property to eliminate the isoclinic parameter when the polariscope is adjusted to circulate polarized light. When the light source is white, the isocromatics are formed by different colorations of luminous bands depending on the fringe order (*N*), as shown in figure 2.

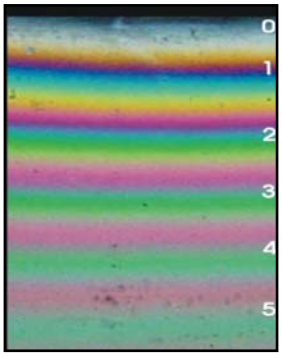

Figure 2. Isocromatic fringe orders.

3. Elliptical Polarized Light

Figure (3) presents the project of a typical polariscope formed by polarizing filters and quarter-wave filters. In this case, the luminous rays spread along of z direction. Depending of the arrangement between the quarter-wave filters and the polarized filters, (plain, circular, or elliptical) polarized light can be obtained. When a transparent model is stressed, phase retardation occurs in the principal stresses direction between the model vectors of emerging light cause by the birefringent effect. The light intensities emergent in the exit of a polarizing plan are given by:

$$I = I_0 \, sen^2 \frac{\delta\pi}{\lambda} sen^2 \, 2(\varphi - \theta) \tag{3}$$

Where *Io* is the maximum value for the light intensities emergent, λ is the wave length, φ is the principal direction angle, θ is the polarization angle, δ is the linear retardation measured in nanometers. That can be written in terms of the angle retardation (Δ) of the following form:

$$\delta = \frac{\Delta\lambda}{2\pi} = N\lambda \tag{4}$$

The equation of the intensity of the emergent light in a polariscope with elliptically polarized light is derived by the calculations from Mueller, Theocaris P. S., Gdoutos E. E., 1979.

The Mueller matrixes for a linear polarizer P_θ with optic axis making an angle θ with the reference axis and the quarter-wave plate $R_\varphi(\Delta)$ with delay Δ, whose fast axis makes an angle φ with the reference axis are expressed by:

$$P_\theta = \frac{1}{2}\begin{bmatrix} 1 & \cos 2\theta & sen\,2\theta & 0 \\ \cos 2\theta & \cos^2 2\theta & \cos 2\theta \, sen\,2\theta & 0 \\ sen\,2\theta & \cos 2\theta \, sen\,2\theta & sen^2\,2\theta & 0 \\ 0 & 0 & 0 & 0 \end{bmatrix} \tag{5}$$

$$R_\varphi = \begin{bmatrix} 1 & 0 & 0 & 0 \\ 0 & \cos^2 2\varphi + \cos\Delta \, sen^2 2\varphi & (1-\cos\delta)\cos 2\varphi \, sen\, 2\varphi & -sen\,\Delta \, sen\, 2\varphi \\ 0 & (1-\cos\Delta)\cos 2\varphi \, sen\, 2\varphi & \cos\Delta\cos^2 2\varphi + sen^2 2\varphi & \cos 2\varphi \, sen\,\Delta \\ 0 & sen\,\Delta \, sen\, 2\varphi & -\cos 2\varphi \, sen\,\Delta & \cos\Delta \end{bmatrix} \tag{6}$$

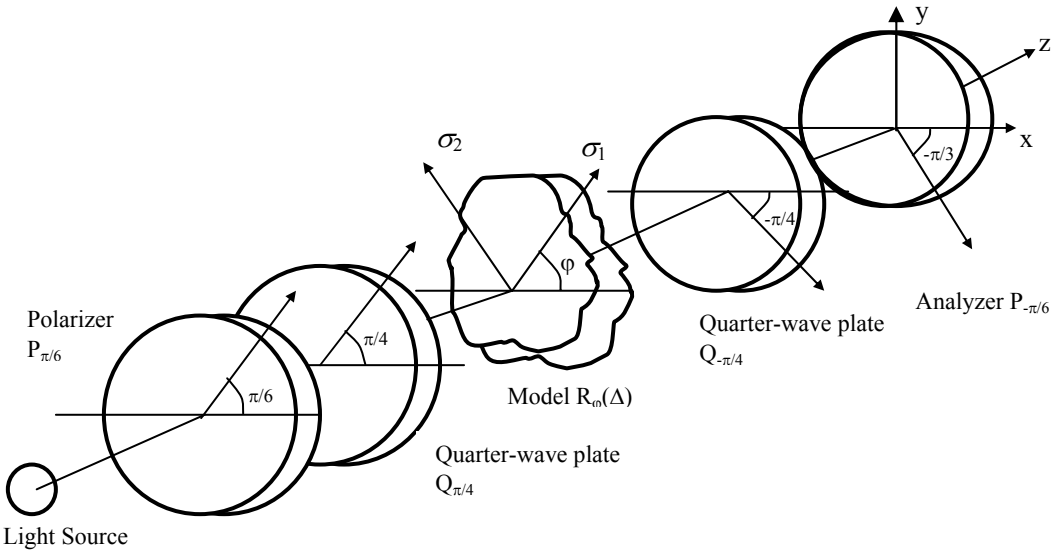

Figure 3. Model placed in a conventional polariscope arrange.

The Mueller matrix of the quarter-wave plate can be obtained substituting $\Delta = \pi/2$ in the Eq. (6). In this work the polarizer and the analyzer axis make angles $\pi/6$ and $-\pi/3$ with relation to x axis and fixed axis of the quarter-wave plates make angles $\pi/4$ and $-\pi/4$ with relation to x axis, respectively. The Mueller matrix of the $\mathbf{P}_{\pi/6}$ polarizer, $\mathbf{P}_{-\pi/3}$ analyzer and wave plates of $\mathbf{Q}_{\pi/4}$ and $\mathbf{Q}_{-\pi/4}$, can be obtained substituting the respective angles in eqs. (5) and (6).

Once the wave plate is modulated for a specific wave length, the additional error in the phase retardation ε is given by:

$$\varepsilon = \frac{\pi}{2}\left(\frac{\lambda_0}{\lambda} - 1\right) \tag{7}$$

Where λ is the wavelength of the used light and λ_0 is the specific wavelength for the quarter-wave plate. The Stokes vector normalized of the non-polarized light emitted is defined as:

$$S = \begin{bmatrix} 1 \\ 0 \\ 0 \\ 0 \end{bmatrix} \tag{8}$$

Following the Mueller calculus, the Stokes vector **S'** of the analyzer emerging light is given by:

$$S' = [P_{-\pi/3} \quad Q_{-\pi/4} \quad R_\varphi(\Delta) \quad Q_{\pi/4} \quad P_{\pi/6}]\, S \tag{9}$$

So, from eqs. (5) to (9) it results:

$$S' = \frac{1}{64}\begin{bmatrix} 2(9+\cos 2\varepsilon + 5\cos 4\varphi + \cos 2\varepsilon + \cos 4\varphi + 4\sqrt{3}\, sen\,\varepsilon \, sen\, 4\varphi)\, sen^2(\Delta/2) \\ (9+\cos 2\varepsilon + 5\cos 4\varphi + \cos 2\varepsilon + \cos 4\varphi + 4\sqrt{3}\, sen\,\varepsilon \, sen\, 4\varphi)\, sen^2(\Delta/2) \\ (9\sqrt{3} + \sqrt{3}\cos\varepsilon + 5\sqrt{3}\cos 4\varphi + \sqrt{3}\cos 2\varepsilon \cos 4\varphi + 12\, sen\,\varepsilon \, sen\, 4\varphi)\, sen^2(\Delta/2) \\ 0 \end{bmatrix} \tag{10}$$

4. Automatic determination of fringe order

The light intensity emerging from the filter of the camera can be expressed as a function of a light intensity parcel defined for Eq. (10) and of optical parameters of the acquired image, being given by:

$$I = I_0 \frac{1}{16} \frac{1}{\lambda_2 - \lambda_1} \int_{\lambda_1}^{\lambda_2} I_0 F_i \, sen^2\left(\frac{\delta \pi C_\lambda}{\lambda C_0}\right)(9 + cos\, 2\varepsilon + 5\, cos\, 4\varphi + cos\, 2\varepsilon\, cos\, 4\varphi + 4\sqrt{3}\, sen\, \varepsilon\, sen\, 4\varphi)d\lambda \tag{11}$$

Where i = r, g, b denote the colors red, green and blue, λi1 and λi2 are the minimum and maximum limits of the filters equipped in the camera and Fi (= Fi(λ)) they are spectral response of the red, green and blue filters.

The error of the quarter-wave plate (ε) and the dispersion of the double refringence are ignored on condition that the effect of these parameters are not very wide. Comparing the values of the light intensity in each point of the model analyzed with the corresponding values in one calibration table, which relates the fringe order with the values of the light intensity (Parameters RGB), the fringe order can be determined.

In the photoelastic technique proposal the fringe orders can be determined by two functions error, defined as:

$$E_j = (R_j - R_m)^2 + (G_j - G_m)^2 + (B_j - B_m)^2 \tag{12}$$

$$Ej = \left(\frac{R_j}{R_j + G_j + B_j} - \frac{R_m}{R_m + G_m + B_m}\right)^2 + \left(\frac{G_j}{R_j + G_j + B_j} - \frac{G_m}{R_m + G_m + B_m}\right)^2 + \left(\frac{B_j}{R_j + G_j + B_j} - \frac{B_m}{R_m + G_m + B_m}\right)^2 \tag{13}$$

Where R_m, G_m and B_m are values of the digitalized lights intensities Ir, Ig and Ib, for example the gray tones of the image in each point and R_j, G_j and B_j are also digitalized values obtained from the calibration table, respectively. The fringe order in each point can be determined through the index (j) that minimizes the function E_j error. The function error defined in eq. (13) is used as complement in the analysis due to the weakness of the elliptical light intensity. Therefore, the analysis of the fringe order can be executed by means of the two functions E_j error, evaluating itself the values of the indices (j) that minimize both functions and modulating the exits through the entire relative indices fringe orders to each relative minimum.

If the variation the fringe order in the calibration table is linear and first pixel of the calibration card is zero in the fringe order, the order of the Nj fringe corresponding to pixel (j) is given by:

$$N_j = N_m \frac{j}{j_m} \tag{14}$$

Where N_m is the maximal fringe order in the calibration table and j_m is the total of values archived in the calibration table.

5. Attainment of the photoelastic models

The methodology will be evaluated through a circular disk under constant compress load. This disk is made of the same photoelastic material. As shown in the previous section, it is necessary to use another phototoelastic model for the attainment of the calibration table. In this in case, the used model was a prismatic bar subjected to a four points bending. Figure 4 shows the dimensions of the models used in the analysis. The photoelastic models were produced from molds made of blue silica rubber. Figure 5 shows the silica molds used to cast the photoelastic models.

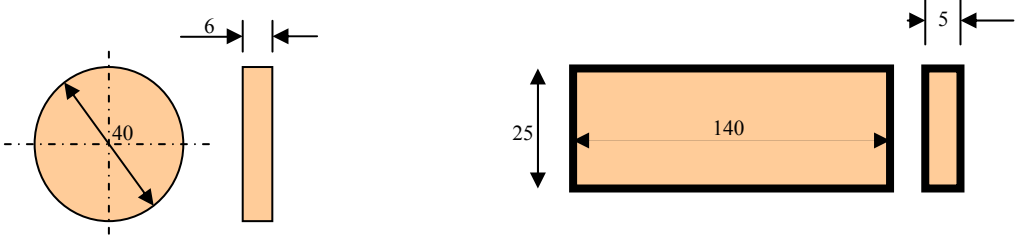

a) Disk under compression b) Calibration beam.

Figure 4. Dimensions of the analyzed models (mm).

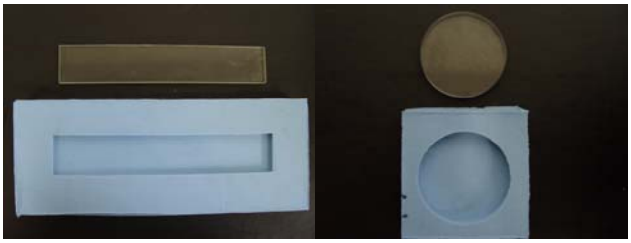

Figure 5. Photoelastics molds.

The photoelastic models were obtained from an epoxy-resin mixture and catalytic agent of the Polipox manufacturer. The ratio volume part of the catalyser (Solution B) was used for two parts in volume of the resin (Solution A), Oliveira (2003). This resin was carefully mixed, approximately 15 minutes, trying to prevent the bubbles formation. The molds fulfilling is made in the room temperature. To follow, they are left in an oven in the temperature of 25 °C during a period of 48 hours in order to complete the cure.

For the accomplishment of experiments, the bar calibration model beam was placed in a polariscope developed in the Mechanical Project Laboratory (MPL) of the College of Mechanical Engineering, being located in a four-point compression load device. The load applied in the model was controlled by means of a Kratos load cell of capacity 50 KN. The optical constant was obtained by a previous calibration process from the work of Araújo, Bernardes and Neves (2004), being of 0.26 N/mm.fr. Despite the constant optics of the used material being low its optical response is excellent, even for small applied load levels. Therefore, in the calibration beam model the load was 15 N generating fringes order of 3 in the model. Figure 6 shows the experimental set up used to get the image and the calibration fringes table. Figure 7 shows the fringes standard obtained in the calibration model.

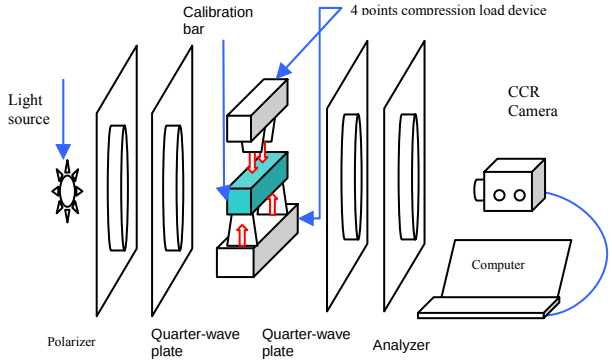

Figure 6. Experimental set up to get the calibration bar image used to mount the fringe calibration table.

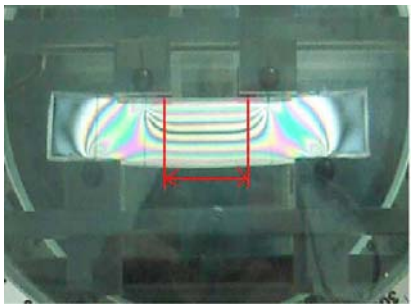

Figure 7. Fringes standard in the central part of the calibration model using polarized elliptical light.

A circular disk loaded in diametral compression was placed in a polariscope with elliptical light for the validation of the technique proposed, under a 10 KN load. The values of fringes images were acquired by a digital camera and transferred directly to the software, developed in Matlab environment. Figure 8 shows the fringes standard of the compressed disk. In a new methodology applied, this disk is used too to calibrate the principal stresses direction (Fig. 9). This calibration is done for minimize the influence of noise images and experimental adjustments errors when the program is calculating the principal directions values.

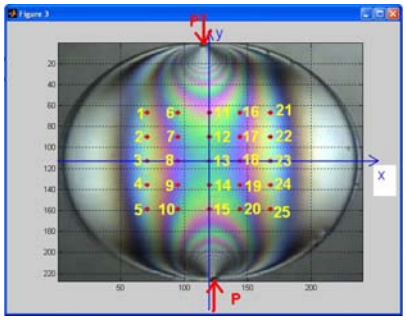

Figure 8. Photoelastic image of the disk under compression of 10 N.

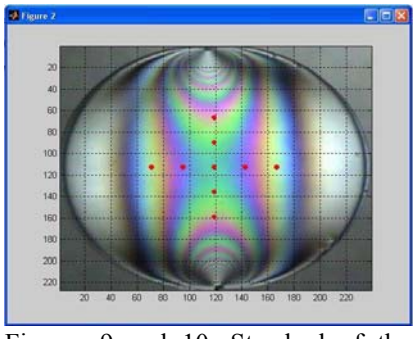

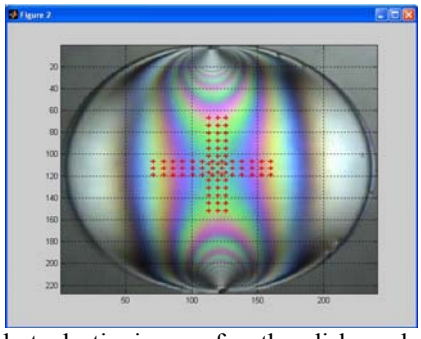

Figures 9 and 10. Standard of the photoelastic image for the disk under compression of 10 N (9 points was used to calibrate the principal stress directions).

The principal stress directions are obtained with the generation of the calibration table and the calibration points. In this work a photoelastic model of plane pillar screw used in dental implants was analyzed. To evaluate the screw preload level was designed the experimental setup composed by the screw head fixed in a base and the gripping pin attached at the load cell. This experimental setup was mounted at the polariscope.

The Fig. 10 shows a pillar implant and the respective screw, the molds obtained and the photoelastic models obtained. The Fig. 11 shows this models set, already prepared and under load in the polariscope. The Fig. 12 shows the photoelastic image of the models set obtained in the polariscope from the MPL/UFU.

Figure 10 – Molds, implant and photoelastic sets generated.

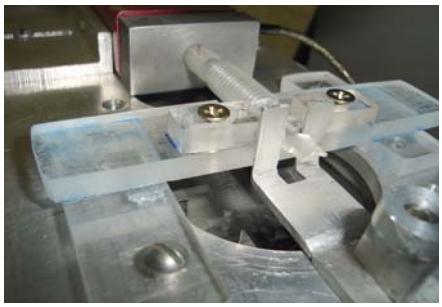

Figure 11 – Models set (plane shape) under load in the polariscope.

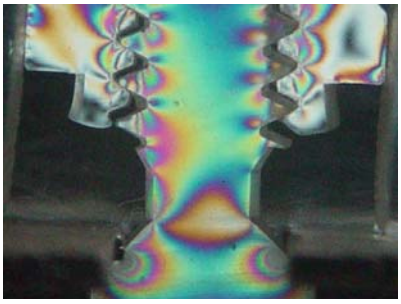

Figure 12 – Photoelastic image of the models taken from the polariscope.

6. Results

The calibration table is generated automatically and the disk image is loaded to be analyzed. A load of 10 N was applied in the disk monitored through a suitable load cell system. In this case, the maximum order fringe of the interest points in the disk were approximately 3, as it shows Fig. 8. The results can be validated experimentally by manual reading using Tardy compensation method and also with the theory (Timoskenko, 1951). This disk was used to validate the method and, in sequence, was used to generate the reference to calculate the principal stresses directions.

For calculate the photoelastic parameters The user then defines how the data will be used in the software. In the disc model, a 25 points grid was created to evaluate the methodology in accordance with the Fig. 8. The Table 1 shows the fringe orders for the analyzed points in the disk under compression and its two solutions for the principal stresses directions. The shear stress (τ) can be obtained by :

$$\tau = \frac{\sigma_1 - \sigma_2}{2} = \frac{NK\sigma}{2b} \tag{15}$$

In the Eq. (15) σ_1 and σ_2 are the principal stresses, with σ_1 being of tensile and σ_2 of compression. Figure 11 shows the calculated maximum shear stress in the models points analyzed, analytically and experimentally and by the software.

Table 1 – Photoelastic parameters obtained for the 25 grid points in the disk model under compression load (10N).

Point Number	Fringe Order	Shear Stress	Solution A		Solution B	
			φ_1	φ_2	φ_1	φ_2
1	1.569	30.86	2.409	87.590	14.932	75.067
2	1.523	29.95	0.793	89.206	13.387	76.612
3	1.476	29.04	0.593	89.406	13.251	76.748
4	1.476	29.04	1.102	88.897	13.758	76.241
5	1.384	27.23	3.304	86.695	16.069	73.930
….						
….						
…						
22	1.569	30.861	2.637	87.362	15.160	74.839
23	1.476	29.046	0.648	89.351	13.011	76.988
24	1.523	29.953	0.135	89.864	13.732	76.267
25	1.523	29.953	2.165	87.834	15.761	74.238

It was verified that the fringe orders obtained by the method in the analyzed points are next to those obtained by the usual method and also through the analytical method. The manual reading was made following standards procedures of fringes analysis considering as 0.5 as being the maximum resolution in the fringe orders. For the analytical models a Matlab program was developed to calculate the stress in x,y directions which were been used to calculate the maximum shear stress. Using the Eq. (15), the analytical fringe orders can be calculated. For some noises in the photoelastic images were observed differences in some analyzed points.

After to obtain the reference to obtain the principal stresses directions from the calibration disk, the software calculates the photoelastic parameters to the model in study. In this case, it was used a photoelastic image from a pillar implant and its screw, like already shown in the Figs. 10, 11 and 12. The Fig. 13 shows 11 points the interest choice for the user to define where the software would obtain the photoelastic parameters.

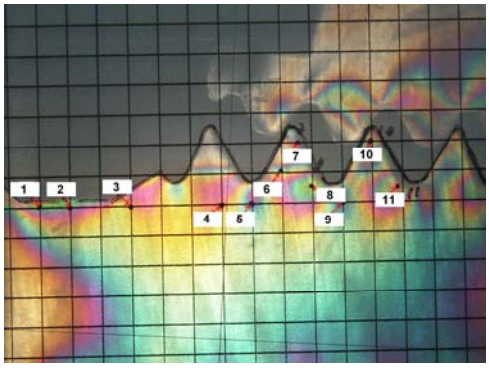

Figure 13 – Partial photoelastic image of the screw and the pillar under load.

Table 2 – Photoelastic parameters in the studied model.

Point Number	Software FRINGES			Experimental		Relative Error (%)
	N	φ_1	φ_2	N	φ_1	N
1	2.6	NC	NC	2.91	5	10.7
2	2.52	NC	NC	2.77	0	9.0
3	2.5	4.1	16.2	2.43	5	2,4
4	2.3	2	14.5	2.43	14	5.3
5	2.2	3.5	15.8	2.47	13	10.9
6	2.55	1.2	13.4	2.32	12	9.0
7	1.37	NC	NC	1.13	32	17.5
8	2.67	1.2	13.5	3.17	11	15.7
9	2.21	1.7	14.4	2.41	12	8.3
10	1.39	NC	NC	1.6	49	13.1
11	2.72	1.3	13.6	3.31	17	17.9

7. Conclusions

The work presents a methodology for obtaining of the photoelastic parameters using polarized elliptical light. The methodology validation was made through a disk under compression load. All the photoelastic models and the experimental apparatus used and the methodology evaluation have been presented. The determination process of the principal stress directions is in progress, as well as refinements in the technique proposed, mainly, through the elimination of images noises. Due to its simplicity of implementation, the applied method can be used of advantageous and efficient form in the photoelasticity technique. The model photoelastic parameters can be obtained automatically through the image acquisition and processing eliminating the inconveniences of a manual reading.

8. References

Araújo, C. A., Neves, F. D., Bernardes, S. R., 2004, "Stress analysis in dental implants using the photoelasticity technique". Proceedings of the 3rd National Congress of Mechanical Engineering, Belém, Brazil.

Dally, J. W., Riley, W. F.,1978, "Experimental Stress Analysis". McGraw–Hill, Inc.

Oliveira, E. J., 2003, "Material e técnica para análise fotoelástica plana da distribuição de tensões produzidas por implantes odontológicos." Dissertação de Mestrado em Reabilitação Oral - Faculdade de Odontologia, Universidade Federal de Uberlândia, Uberlândia, Brazil.

Pindera J. T., Cloud G., 1966, "On dispersion of birefringent of photoelastic materials", Exp. Mech., pp. 470–80.

Takashi M., Mawatari S., Toyoda Y., Kunio T., 1990, "A new computer aided system for photoelastic stress analysis with structure-driven type image processing." In Applied stress analysis, Elsevier Applied Sciences, London, pp. 516-525.

Timoshenko S. P., Goodier J. N., 1970, "Theory of elasticity", 3rd. ed. MacGraw-Hill Inc., New York.

Theocaris P. S., Gdoutos E.E, 1979, "Matrix Theory of Photoelasticity", Proceedings of Springer–Verlag, New York.

Yoneyama, S., Takashi, M., 1998, "A new method for photoelastic fringe analysis from a single image using elliptically polarized white light", Optics and Lasers in Engineering, V 30, pp. 441–459.

9. Responsibility notice

The authors are the only responsibles for the printed material included in this paper.